CrossMark

ORIGINAL ARTICLE

Diagnostic utility of a computer-aided diagnosis system for whole-body bone scintigraphy to detect bone metastasis in breast cancer patients

Misugi Urano[1] · **Yumi Maki**[1] · **Hiroko Nishikawa**[1] · **Tatsuya Kawai**[1] ·
Norio Shiraki[2] · **Yuta Shibamoto**[1]

Abstract

Objective To compare the diagnostic ability of planar images (PI) and images obtained by a computer-aided diagnosis (CAD) system (Viewer for Standardized Bone Scintigraphies; VSBONE) of whole-body bone scintigraphy for detecting bone metastases in breast cancer patients.
Methods 81 women (median: 56 years; range: 32–79) with a history of breast cancer were included in this study. They underwent whole-body bone scintigraphy after intravenous injection of 740 MBq technetium-99m hydroxymethylene diphosphonate. A total of 1066 bones (162 regions of the skull, 657 regions of the spine and pelvis, 223 regions of the sternum and rib, 18 regions of the upper extremities, and 6 regions of the lower extremities) were analyzed. The PI alone, VSBONE images alone, and both PI and VSBONE images (PI + VSBONE) were interpreted independently by two radiologists to diagnose bone metastases, which were then confirmed by magnetic resonance imaging. The sensitivity and specificity for each modality were analyzed using Fisher's exact and McNemar tests. Inter-reviewer agreement was evaluated using a kappa statistic.
Results Bone metastases were confirmed in 43 patients with 442 positive lesions. The average sensitivity of PI, VSBONE images, and PI + VSBONE images was 40.8, 50.2, and 61.8 %, respectively. The average specificity was 97.8, 97.5, and 97.6 %, respectively. The kappa scores were 0.62 for PI, 0.69 for VSBONE, and 0.77 for PI + VSBONE.
Conclusions VSBONE was superior to PI in regard to sensitivity for detecting bone metastases in breast cancer patients. However, an improved CAD system is required to decrease the number of false-negative results.

Keywords Breast cancer · Metastases screening · Bone scintigraphy · CAD

Introduction

Patients with advanced breast cancer frequently develop bone metastases, and the extent of the disease significantly affects overall survival [1]. Bone metastasis also causes skeletal-related events (SREs), including pain, bone fractures, spinal cord compression, and hypercalcemia. SREs significantly impair patients' quality of life [2]. Zoledronic acid and other bisphosphonates have been shown to reduce the risk of SREs in breast cancer patients with bone metastasis [3]. Radiation therapy has also been shown to be effective in countering bone metastases from breast cancer [4]. Thus, the early diagnosis of bone metastasis is important to choose an appropriate treatment.

Bone scintigraphy is an effective diagnostic tool for whole-body examination of bone metastases [5, 6]. It is used to evaluate the extent of metastatic spread in bone tissue for both staging and follow-up [1, 7, 8]. However, the interpretation of bone scintigraphy images is a difficult pattern-recognition task that requires extensive experience [9]. Because non-neoplastic diseases can also exhibit abnormalities on imaging findings, a number of different diagnoses and possible error sources should be considered [10]. Therefore, physicians must be able to read the diagnostic images carefully and avoid

✉ Misugi Urano
  koremicchannodakara@yahoo.co.jp

1 Department of Radiology, Nagoya City University Graduate School of Medical Sciences, Kawasumi 1, Mizuho-ku, Nagoya, Aichi 4678601, Japan

2 Department of Radiology, Nagoya City West Medical Center, 1-1-1, Hirate-cho, Kita-ku, Nagoya 462-8508, Japan

errors in interpretation that could lead to serious mistakes in the treatment of patients [9].

The computer-aided diagnosis (CAD) system (Viewer for Standardized Bone Scintigraphies: VSBONE) was developed by Nihon Medi-Physics Co., Ltd. (Tokyo, Japan) for the purpose of improving the detectability of interval changes in successive whole-body bone scintigraphy. To detect interval changes, the gray scale of each image is first normalized, and then, the body size, body position, and gray-scale density of the first image are adjusted to match those of the second image [11]. Because there is no literature regarding the effectiveness of VSBONE to our knowledge, we examined the diagnostic ability of VSBONE to detect interval changes in repeated whole-body bone scintigraphies and compared these images to the ability of the conventional planar images (PI) to detect bone metastases in breast cancer patients.

Patients and methods

Patients

Between January 2004 and June 2016, 747 women with breast cancer underwent whole-body bone scintigraphy at our institution, and 272 of them underwent subsequent whole-body bone scintigraphy at intervals of more than 2 months. Among these women, 81 patients (median: 56 years; range: 32–79) who had undergone magnetic resonance imaging (MRI) at the suspected lesion levels within 3 months (median: 20 days; range: 0–89) of the second whole-body bone scintigraphy were included in this study. The patient and tumor characteristics are shown in Table 1. A total of 1066 bones (162 regions of the skull, 657 regions of the spine and pelvis, 223 regions of the sternum and rib, 18 regions of the upper extremities, and 6 regions of the lower extremities) were analyzed in this study (Table 2). This retrospective study was approved by the ethics committee of our institution, and informed consent from each patient was waived.

Bone scintigraphy

Patients underwent whole-body bone scintigraphy 3 h after intravenous injection of 740 MBq (20 mCi) technetium-

Table 1 Patients and characteristics

Clinical T factor	T1/2/3/4/Unknown	22/34/9/5/11
Clinical N factor	N0/1/2/3/Unknown	34/27/5/4/11
Histological type	IDC/ILC/Other/unknown	68/2/3/8

IDC invasive ductal carcinoma, *ILC* invasive lobular carcinoma, *Other* 2 mucinous carcinomas and 1 apocrine carcinoma

Table 2 Number of bone metastases in each bone segment

Bone segments	Bone segments (no.)	Bone segments with metastases (no.)
Skull	162	31
Cervical spine	101	54
Thoracic spine	353	205
Lumbar spine	157	111
Sacrum with coccyx	34	22
Pelvis	12	6
Sternum	2	0
Ribs	221	10
Upper extremities	18	0
Lower extremities	6	3
Total	1066	442

99m-hydroxymethylene diphosphonate (Tc99m-HMDP; Nihon Medi-Physics). Whole-body images (anterior and posterior views, scan speed 20 cm/min, and matrix 256 × 1024 or 768 × 512) were obtained with a gamma camera (e.cam; Siemens, Forchheim, Germany or Bright View X with XCT; Philips, Best, The Netherlands) equipped with low-energy high-resolution parallel hole collimators. Energy discrimination was provided by a 20 % window centered at 140 keV of Tc99m. PIs of the entire skeleton in the anterior and posterior positions were acquired. No single-photon emission computed tomography (SPECT) was used in this analysis.

Initial bone scintigraphy was performed as a part of the staging procedure after the diagnosis of breast cancer or to screen for causes of pain. The second bone scintigraphy was performed to assess any changes of known metastases annually or to examine new lesions when pain symptoms and/or increases in tumor markers (CEA, CA15-3, BCA225, and/or NCC-ST-439) were noted. The interval between the initial and second scans was 3–113 months (median, 26 months).

Diagnostic supporting software analysis

All the raw data of bone scintigrams were sent to and stocked in the PACS database. For the present study, we used the special diagnostic supporting software VSBONE version 1.5 to analyze bone scintigraphy [11]. The raw data in a DICOM format of each patient were exported from the PACS database to a workstation for VSBONE analysis. With this software, the anatomical structures were analyzed using the raw data obtained by the initial and second bone scans, and then, the gray-scale density, body size, and position of the body were normalized. As a result, adjusted bone scintigrams were generated for both anterior and posterior images (Fig. 1).
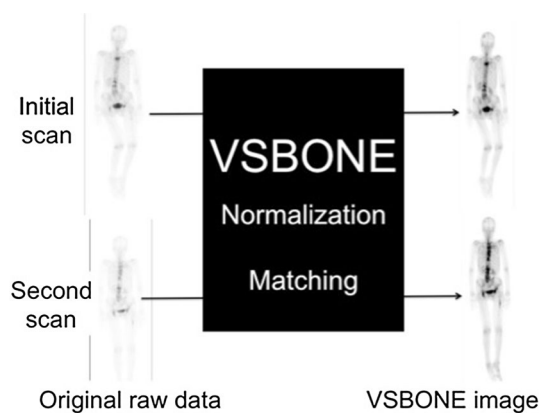
Fig. 1 Example of planar bone scintigraphy images and images processed by VSBONE for the posterior view. Initial and second original raw image data were compared and analyzed as planar images. The *gray scale* of the initial and second images was normalized first, and then, the size, orientation, and *gray scale* of the initial images were referenced to match those of the second images

MR imaging and criteria for bone metastasis

MR studies were scheduled for screening of pain symptoms or confirming metastatic lesions suspected by bone scintigraphy or CT. MR studies were performed for one or a few painful or suspected regions, and no patient underwent whole-body MRI in this study. Brain, breast, and other MR examinations were also analyzed when the suspected bone lesions were evaluable on the MR images. All MR studies were performed on 1.5- or 3.0-Tesla scanners. For all patients, we performed the standard techniques with T1-, T2-weighted images (T1WI, T2WI), and at least one of the following sequences: short-tau inversion recovery (STIR), fat-suppressed T2WI, spectral pre-saturation with inversion recovery (SPIR), and spectral attenuated inversion recovery (SPAIR) sequences.

Contrast-enhanced MR studies were recommended whenever possible following unenhanced scans. However, more than half of these patients could not undergo enhanced MRI because of booking limitations, renal disorder or other reasons. The criteria for the MRI diagnosis of metastasis were the presence of a well-defined focus of low signals on both T1WI and T2WI and/or a high signal intensity on fat-suppressed T2WI.

Image analysis

The PI alone, VSBONE images alone, and both PI and VSBONE images (PI + VSBONE) were interpreted separately by two independent radiologists with 6 and 14 years of experience, respectively, to diagnose bone metastases. The two radiologists were fully blinded to any clinical information, including levels of tumor markers, such as CEA, CA15-3, BCA225, and NCC-ST-439. They

performed three reading sessions. These sessions were spaced at least 4 weeks apart. The reviewers were free to use tools, such as zooming and adjusting window width and/or level while reading PI. With reference to each initial bone scintigraphy, the second bone scintigraphy was assessed qualitatively for changes in the lesions present on the initial bone scintigraphy and for the presence of new lesions. For all 1066 regions, every site with an abnormal uptake of 99mTc-HMDP was recorded by region as positive or negative for metastatic involvement.

On bone scintigraphy, the presence of abnormal uptakes except apparent benign changes was considered as the positive finding for bone metastasis. Bone metastases and benign changes were differentiated based on the shape and distribution of the abnormal uptake. For example, a round-shaped uptake in a rib was diagnosed as benign changes, whereas an extended uptake was considered to indicate malignant change. A joint-based uptake in the vertebrae and a typical uptake by an arthritic or degenerative change were diagnosed as benign uptakes, whereas uptakes in the center of the vertebrae and multiple random uptakes in the vertebra were judged as metastases. "The beautiful bone scan" and clear cold spots were also judged as metastases.

The MR diagnosis of metastasis was made blindly by two radiologists with 17 and 8 years of experience, respectively, who were fully blinded to any clinical information, including levels of tumor markers, such as CEA, CA 15-3, BCA 225, and NCC-ST-439 in consensus for all 43 patients; this diagnosis was used as the gold standard for the presence or absence of bone metastasis.

Statistical analysis

To compare the sensitivity and specificity of PI and VSBONE for determining the presence of the metastatic involvement of bones, the Fisher exact and McNemar tests were performed. Inter-observer agreement was calculated using kappa statistics. Kappa scores of 0.41–0.60, 0.61–0.80, and greater than 0.80 were regarded to be indicative of moderate, good, and excellent agreement, respectively [12].

Results

Bone metastases were confirmed in 43 patients with 442 positive lesions (Table 2). Table 3 shows the number of true-positive and true-negative lesions, sensitivity, and specificity of detection of metastatic bone involvement by each reviewer. The average sensitivity of PI, VSBONE, and PI + VSBONE images was 40.8, 50.2, and 61.8 %, respectively. The average specificity was 97.8, 97.5, and 97.6 %, respectively. The sensitivity of the VSBONE

Table 3 Sensitivity and specificity of planar images and VSBONE

| | | No. (%) of cases | | | |
		Planar images	VSBONE	P^*	P^{**}
Reviewer 1	Sensitivity	188/442 (42.5)	223/442 (50.5)	0.02	0.0005
	Specificity	608/624 (97.4)	608/624 (97.4)	>0.99	
Reviewer 2	Sensitivity	173/442 (39.1)	221/442 (50.0)	0.0015	<0.0001
	Specificity	613/624 (98.2)	609/624 (97.6)	0.55	

* Fisher's exact test, ** McNemar test

Table 4 Sensitivity and specificity of planar images and planar images + VSBONE

		No. (%) of cases Planar images + VSBONE
Reviewer 1	Sensitivity	251/442 (56.8)
	Specificity	609/624 (97.6)
Reviewer 2	Sensitivity	295/442 (66.7)
	Specificity	609/624 (97.6)

images was better than that of PI for both reviewers. In addition, there were significant overall differences between PI and VSBONE in diagnosing bone metastases for both reviewers. The average number of false-positive lesions was 5, 10, and 10 in of PI, VSBONE and PI + VSBONE, respectively. The average PPV was 97, 95, and 96 %, respectively (Table 4).

The kappa scores for agreement between the reviewers were 0.62 for PI, 0.69 for VSBONE, and 0.77 for PI + VSBONE. Agreement could, therefore, be considered good for PI, VSBONE, and PI + VSBONE. Figure 2 shows a 60-year-old breast cancer patient. On initial bone scintigraphy images, there were no abnormal uptakes (Fig. 2, left panels). Seven years and 6 months after the initial bone scintigraphy, she complained of neck pain, lumbago, and coxalgia. She then underwent a second bone scintigraphy (Fig. 2, right panels). Reviewer 1 interpreted lesions in C1, T10, T11, L3, and L4 on PI and in C1, T9-11, L3, and L4 on VSBONE as metastases. Reviewer 2 interpreted T11, L3, and L4 lesions on PI and T9, T11, L3, and L4 lesions on VSBONE as metastases. Reviewer 2 diagnosed a hot spot in the C1 lesion as a joint-based uptake or degenerative change. On the MRI, metastatic lesions of C1, C6, T1, T3, T6, T7, T9-11, L1, and L3-5 were confirmed (Fig. 3).

Discussion

Bone scintigraphy is an important diagnostic tool for detecting and monitoring bone metastases in patients with advanced breast cancer, because it is widely available and
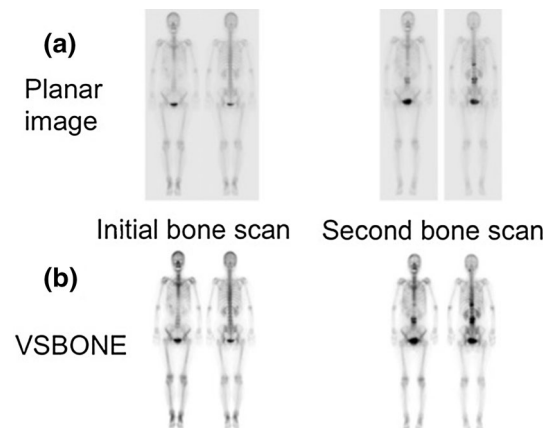

Fig. 2 60-year-old female who underwent left mastectomy 20 years ago. The initial bone scintigraphy was performed for screening. She complained of neck pain, lumbago, and coxalgia, for which the second scintigraphy was performed 7 years and 6 months after the initial scan. **a** Initial PI showed no metastatic lesion. The second PI showed three obvious foci of uptake. The lesions at T11, L3, and 4 were interpreted as metastases by both reviewers. The lesions at C1 and T10 showed equivocal uptake. One reviewer interpreted these as metastases, but the other did not. **b** Initial VSBONE images showed no obvious metastatic lesion. The second VSBONE images showed four obvious foci. The lesions at T11, L3, and 4 were interpreted as metastases by both reviewers. The lesion at C1 was interpreted as a metastasis by reviewer 1 and a benign lesion by reviewer 2. The lesions at T9 and 10 showed equivocal uptake. The T9 lesion was interpreted as a metastasis by both reviewers. The T10 lesion was interpreted as a metastasis by reviewer 1 and a benign lesion by reviewer 2

provides an entire skeletal visualization within a reasonable amount of time and at a reasonable cost [13]. Bone scintigraphy, PET-CT, and MRI can screen the whole body, but due to the high cost and/or long duration of a whole-body study, PET-CT and MRI cannot be routinely used as a standard procedure for follow-up [1, 13]. For that reason, bone scintigraphy is a universal tool that has the possibility to detect unexpected bone metastasis and facilitate an early diagnosis. However, one of the major drawbacks of the conventional bone scintigraphy is the high subjectivity when evaluating target bone regions [14]. In this study, the sensitivity and kappa score of VSBONE and PI + VSBONE for the diagnosis of bone metastases were higher than those of the conventional PI. For PI, the
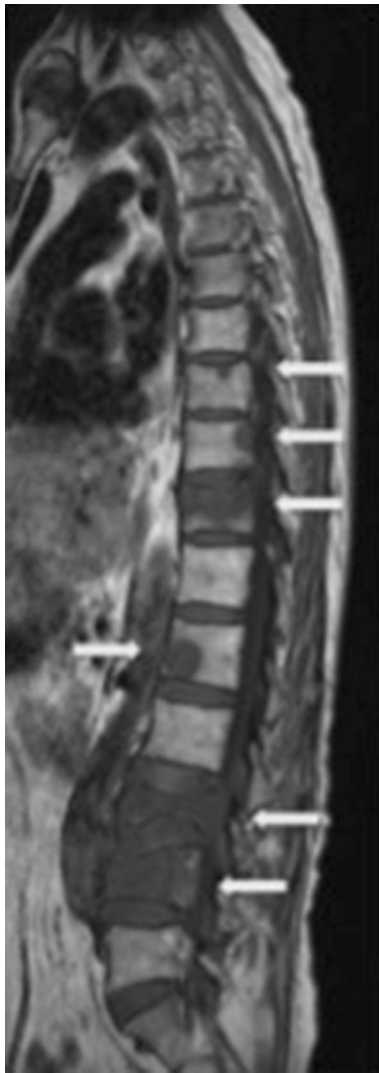
Fig. 3 Same patient as shown in Fig. 2. T1-weighted sagittal images show low signal-intensity mass lesions in C1, C6, T1, T3, T6, T7, T9-11, L1, and L3-5 corresponding to bone metastases (*arrows* partly not shown)

fine gray-scale adjustment was dependent on each observer. It is difficult to diagnose subtle uptake with the low resolution of scintigraphy images. VSBONE can correct the variations in image gray scales and in geometric image features for gray-scale normalization and image matching, respectively [11]. Thus, the VSBONE images could reduce the false-negative cases caused by this standardization.

In this study, the two reviewers diagnosed bone metastases using bone scintigraphies without patients' medical records, MRI, CT, or other radiographic images, because bone scintigraphy is the first choice for screening owing to its utility and ability to evaluate the entire skeleton at low cost [15]. We used the MRI findings as the gold standard for the presence or absence of bone metastases, because MRI is known to be much more sensitive for detecting

bone lesions than bone scintigraphy or CT. The diagnostic superiority of MRI over bone scintigraphy for identifying secondary bone lesions has been demonstrated convincingly by many authors [16–18].

Bone metastases from breast cancer can be osteoblastic, osteolytic, or mixed [9], and bone scintigrams are sensitive in detecting any changes in osseous metabolism [19]. Tokuda et al. [9] reported a retrospective analysis of CAD for bone scans in 109 patients with breast cancer. The sensitivity and specificity were 83.3 and 67.8 %, respectively. Their gold standard of determining the presence or absence of bone metastases was based on any available diagnostic MRI, CT, or radiographic images, and anatomical regions were not considered. Because of these reasons, the sensitivity of both the conventional bone scintigraphy and the VSBONE might have been lower in our study than in the past studies.

To improve the diagnostic ability of bone scintigraphy, several other technical methods are being developed. VSBONE is one of the CAD systems for diagnosing follow-up bone scintigraphy images in comparison with the past images. It can standardize density, display parallel images, and set any quantitative value, and is easy to handle. Until recently, the VSBONE software was included in a software File Manager and Launcher Components for Nuclear Medicine (Nihon Medi-Physics), and could be obtained without charge from the company. However, it is now included in a commercial software, AZE Virtual Place HAYABUSA (AZE, Ltd., Tokyo, Japan). The special CAD system "BONENAVI" (Fujifilm RI Pharma Co., Ltd., Tokyo, Japan) has recently been reported to be useful for diagnosing bone metastases via bone scintigraphy in breast cancer patients [9, 14, 19]. Both CAD systems can compare the first and successive data. Patients with advanced breast cancer developing bone metastases can survive for long periods with appropriate treatments [1], and so for appropriate management of bone metastases, storing the raw data for a long time is important, although somewhat inconvenient. Using these raw data, both VSBONE and BONE-NAVI can show the adjusted images. Comparisons between VSBONE and this new method, and the potential benefits of their combinations, should be topics of future investigations. The addition of SPECT or SPECT/CT to the acquisition protocol of bone scintigraphy could improve its diagnostic accuracy and sensitivity for detecting malignant bone involvement [13, 16, 17, 20].

Our study had several limitations. As the total number of cases was relatively small and the follow-up period was not sufficiently long in some patients, the rate of bone metastases might change as the number of patients and follow-up period increase. A multicenter study will also be needed to address issues, such as differences in the interpretation style at different clinics and differences in the incidence of

metastatic disease. Thus, the accumulation of more cases is necessary. In addition, we did not consider the flare phenomenon on bone scintigraphy [21]. Furthermore, there were many false-negative lesions when diagnosed using VSBONE alone. Referring to other imaging modalities, such as MRI, CT, and PET-CT, would increase the accuracy of diagnosis in the clinical setting [13]. Despite these limitations, this is the first report to show a promising role for VSBONE in the evaluation of bone metastases for patients with breast cancer.

Conclusions

The sensitivity and kappa score of VSBONE were higher than those of PI for detecting bone metastases in breast cancer patients. Although further improvement of the computerized scheme would be necessary to reduce the number of false-negative diagnoses, the CAD scheme for detecting interval changes using the temporal subtraction technique would be useful in assisting radiologists' interpretations of successive bone scintigraphy images.

Compliance with ethical standards

Conflict of interest　No authors have any conflicts of interest.

References

1. Maffioli L, Florimonte L, Pagani L, Butti I, Roca I. Current role of bone scan with phosphonates in the follow-up of breast cancer. Eur J Nucl Med Mol Imaging. 2004;31:143–8.
2. Hayashi N, Yamauchi H, Nakamura S. Management of bone metastases from breast cancer. Gan To Kagaku Ryoho. 2012;39:1174–7.
3. Costa L. Bisphosphonates: reducing the risk of skeletal complications from bone metastasis. Breast. 2007;16:16–20.
4. Jeremic B, Shibamoto Y, Acimovic L, Milicic B, Milisavljevic S, Nikolic N, et al. A randomized trial of three single-dose radiation therapy regimens in the treatment of metastatic bone pain. Int J Radiat Oncol Biol Phys. 1998;42:161–7.
5. Duo J, Han X, Zhang L, Wang G, Ma Y, Yang Y. Comparison of FDG PET/CT and gadolinium-enhanced MRI for the detection of bone metastases in patients with cancer: a meta-analysis. Clin Nucl Med. 2013;38:343–8.
6. Shen CT, Qiu ZL, Han TT, Luo QY. Performance of 18F-fluoride PET or PET/CT for the detection of bone metastases: a meta-analysis. Clin Nucl Med. 2015;40:103–10.
7. Brennan ME, Houssami N. Evaluation of the evidence on staging imaging for detection of asymptomatic distant metastases in newly diagnosed breast cancer. Breast. 2012;21:112–23.
8. Azad GK, Taylor B, Rubello D, Colletti PM, Goh V, Cook GJ. Molecular and functional imaging of bone metastases in breast and prostate cancers: an overview. Clin Nucl Med. 2016;41:e44–50.
9. Tokuda O, Harada Y, Ohishi Y, Matsunaga N, Edenbrandt L. Investigation of computer-aided diagnosis system for bone scans: a retrospective analysis in 406 patients. Ann Nucl Med. 2014;28:329–39.
10. Bombardieri E, Aktolun C, Baum RP, Bishof-Delaloye A, Buscombe J, Chatal JF, et al. Bone scintigraphy procedures guidelines for tumor imaging. Eur J Nucl Med Mol Imaging. 2003;30:107–14.
11. Shiraishi J, Li Q, Appelbaum D, Pu Y, Doi K. Development of a computer-aided diagnostic scheme for detection of interval changes in successive whole-body bone scans. J Digit Imaging. 2011;24:680–7.
12. Landis JR, Koch CG. The measurement of observer agreement for categorical data. Biometrics. 1977;33:9–74.
13. Liu T, Cheng T, Xu W, Yan WL, Liu J, Yang HL. A meta-analysis of 18FDG-PET, MRI and bone scintigraphy for diagnosis of bone metastases in patients with breast cancer. Skelet Radiol. 2011;40:523–31.
14. Mitsui Y, Shiina H, Yamamoto Y, Haramoto M, Arichi N, Yasumoto H, et al. Prediction of survival benefit using an automated bone scan index in patients with castration-resistant prostate cancer. BJU Int. 2012;110:628–34.
15. Niikura N, Hashimoto J, Kazama T, Koizumi J, Ogiya R, Terao M, et al. Diagnostic performance of 18F-fluorodeoxyglucose PET/CT and bone scintigraphy in breast cancer patients with suspected bone metastasis. Breast Cancer. 2015. doi:10.1007/s12282-015-0621-z.
16. Even-Sapir E, Metser U, Mishani E, Lievshitz G, Lerman H, Leibovitch I. The detection of bone metastases in patients with high-risk prostate cancer: ^{99m}Tc-MDP planar bone scintigraphy, single- and multi-field-of-view SPECT, 18F-Fluoride PET, and 18F-Fluoride PET/CT. J Nucl Med. 2006;47:287–97.
17. Jambor I, Kuisma A, Ramadan S, Huovinen R, Sandell M, Kajander S, et al. Prospective evaluation of planar bone scintigraphy, SPECT, SPECT/CT, 18F-NaF PET/CT and whole body 1.5T MRI, including DWI, for the detection of bone metastases in high risk breast and prostate cancer patients: SKELETA clinical trial. Acta Oncol. 2015;2:1–9.
18. Engelhard K, Hollenbach HP, Wohlfart K, von Imhoff E, Fellner FA. Comparison of whole-body MRI with automatic moving table technique and bone scintigraphy for screening for bone metastases in patients with breast cancer. Eur Radiol. 2004;14:99–105.
19. Koizumi M, Miyaji N, Murata T, Motegi K, Miwa K, Koyama M, et al. Evaluation of a computer-assisted diagnosis system, BONENAVI version 2, for bone scintigraphy in cancer patients in a routine clinical setting. Ann Nucl Med. 2015;29:138–48.
20. Sharma P, Singh H, Kumar R, Bal C, Thulkar S, Seenu V, Malhotra A. Bone scintigraphy in breast cancer: added value of hybrid SPECT-CT and its impact on patient management. Nucl Med Commun. 2012;33:139–47.
21. Janicek MJ, Hayes DF, Kaplan WD. Healing flare in skeletal metastases from breast cancer. Radiology. 1994;192:201–4.